Article

Identification of a novel effector domain of BIN1 for cancer suppression

Greta L. Lundgaard[2,6#], Natae E. Daniels[2,7#], Slovénie Pyndiah[1,8], Erica K. Cassimere[1,3,9], Kazi M. Ahmed[2,10], Amélie Rodrigue[3,11], Daisuke Kihara[4,5], Carol B. Post[2], and Daitoku Sakamuro[1,2,3]*

[1]Molecular Signaling Program, Stanley S. Scott Cancer Center and Department of Pathology, Louisiana State University Health Sciences Center, New Orleans, Louisiana 70112, USA; Departments of [2]Medicinal Chemistry and Molecular Pharmacology, [3]Biochemistry and Molecular Biology, [4]Biological Sciences, and [5]Computer Sciences, Purdue University, West Lafayette, Indiana 47907, USA

Running Title: Novel growth-inhibitory domain of BIN1

***Correspondence to:** Daitoku Sakamuro, E-mail: dsakam@lsuhsc.edu

[#] These authors contributed equally to this work.

Additional Supporting Information may be found in the online version of this article.

Received 19 April 2011; Revised 16 May 2011; Accepted 3 June 2011
Journal of Cellular Biochemistry

DOI 10.1002/jcb.23222

Current addresses

[6)] High Throughput Biology Group, Gilead Sciences Ltd., Foster City, California 94404, USA greta.lundgaard@gilead.com

[7)] Department of Trait Genetics and Technologies, Dow AgroSciences, Indianapolis, Indiana 46268, USA nedaniels@dow.com

[8)] Hôpital St. Louis, Institut de Génétique Moléculaire, Cibles Thérapeutiques, INSERM U940, F-75010 Paris, France slovenie.pyndiah@inserm.fr

[9)] Department of Integrative Biology and Pharmacology, University of Texas Health Science Center, Houston, Texas 77030, USA Erica.Cassimere@uth.tmc.edu

[10)] Department of Cancer and DNA Damage Responses, Ernest Orlando Lawrence Berkeley National Laboratory, Berkeley, California 94710, USA kmahmed@lbl.gov

[11)] Genome Stability Laboratory, Laval University Cancer Research Center, Québec City, Canada amelie.rodrigue@crchuq.ulaval.ca

Abbreviations

BAR (BIN-Amphiphysin-Rvs-related)

MBD (MYC-binding domain)

MID (MYC-independent effector domain)

Abstract

Bridging integrator 1 (BIN1) is a nucleocytoplasmic adaptor protein with tumor suppressor properties. The protein interacts with and inhibits the c-MYC transcription factor through the BIN1 MYC-binding domain (MBD). However, *in vitro* colony formation assays have clearly demonstrated that the MBD is not essential for BIN1-mediated growth arrest. We hypothesized that BIN1 contains a MYC-independent effector domain (MID) for cancer suppression. Because a functionally unique domain frequently contains a distinct structure, the human full-length BIN1 protein was subjected to limited trypsin digestion and the digested peptides were analyzed with Edman sequencing and mass spectrometry. We identified a trypsin-resistant peptide that corresponds to amino acids 146–268 of BIN1. It encompassed part of the BAR region, a putative effector region of BIN1. Computational analysis predicted that the peptide is very likely to exhibit coiled-coil motifs, implying a potential role for this region in sustaining the BIN1 structure and function. Like MBD-deleted BIN1, the trypsin-resistant peptide of BIN1 was predominantly present in the cytoplasm and was sufficient to inhibit cancer growth, regardless of dysregulated c-MYC activity. Our results suggest that the coiled-coil BIN1 BAR peptide encodes a novel BIN1 MID domain, through which BIN1 acts as a MYC-independent cancer suppressor.

Key words: BIN1, c-MYC, limited proteolysis, cancer suppression, cytoplasmic localization

Introduction

Bridging integrator 1 (BIN1, also known as Box-dependent myc-interacting protein 1) is the member of the BAR (BIN/amphiphysin/Rvs-related) protein family (Sakamuro *et al.,* 1996; Prendergast *et al.,* 2009). Acting through the MYC-binding domain (MBD), which is unique to BIN1, BIN1 interacts with the c-MYC transcription factor and inhibits c-MYC–mediated transactivation and transformation (Sakamuro *et al.,* 1996; Sakamuro and Prendergast 1999). The deletion of the MBD region leads to a failure of the BIN1 protein to inhibit oncogenic properties of c-MYC. In contrast, the ectopically expressed MBD peptide is sufficient to disrupt endogenous BIN1–c-MYC interaction, thereby releasing oncogenic c-MYC activity *in vivo* (Sakamuro *et al.,* 1996; Elliott *et al.,* 1999; DuHadaway *et al.,* 2001). Moreover, the C-terminal SH3 domain of BIN1, which exists adjacent to the MBD, has been identified as an extra BIN1 region involved in physical BIN1–c-MYC interaction (Pineda-Lucena *et al.,* 2005). These results suggest that BIN1 interacts directly with and suppresses the oncogenic activity of c-MYC.

Since the original discovery, a MYC-independent BIN1 activity in tumor suppression has also been indicated (Sakamuro *et al.,* 1996; Elliott *et al.,* 1999). For example, overexpression of the MBD-deleted BIN1 (BIN1ΔMBD) polypeptide, which does not inhibit c-MYC, attenuates oncogenic RAS cotransformation mediated by a non-MYC nuclear oncoprotein, such as adenovirus E1A or dominant-negative mutant p53, in primary rodent fibroblasts (Sakamuro *et al.,* 1996; Elliott *et al.,* 1999; Kinney *et al.,* 2008). Furthermore, similar to the full-length BIN1, transfection of the BIN1ΔMBD inhibits colony-forming activities of various human cancer cell lines (Sakamuro *et al.,* 1996; Elliott *et al.,* 1999). These results suggest that BIN1 exerts its cancer

suppression function by both a MYC-dependent mechanism and a MYC-independent mechanism. However, the entity of the BIN1 MYC-independent effector domain (MID) for cancer suppression remains unknown.

Identification of a naturally folded domain structure may facilitate the identification of the cellular function of a protein of interest or its signaling pathways. For this purpose, limited proteolysis is probably one of the most reliable and relevant methods (Fontana *et al.,* 1997). Potential cleavage sites may be sensitive to limited protease activity, if located within flexible linker regions. In contrast, possible proteolytic sites may remain resistant to limited digestion if they are embedded within a folded domain. Ideally, under optimized proteolytic conditions, cleavage should occur only at flexible linker regions between individually folded domains. Thus, a peptide resistant to limited protease digestion is likely to retain a naturally folded structure. This technique has been used to establish domain structures of a number of enzymes and signaling proteins, such as poly(ADP-ribose) polymerase 1 (PARP1) (Kameshita *et al.,* 1986), cytochrome c (Fontana *et al.,* 1995), breast cancer type 1 susceptibility protein (BRCA1) (Brzovic *et al.,* 1998), and histone deacetylase 1 (HDAC1) (Kamath *et al.,* 2006).

In this study, we undertook limited tryptic digestion of the human full-length BIN1 recombinant protein and determined the structure and function of a trypsin-resistant BIN1 peptide. Our results suggest that the trypsin-resistant peptide *per se*, which encodes part of the BIN1 BAR domain, contains a tightly coiled-coil motif and exists in the cytoplasm. Of note, the peptide is sufficient to inhibit tumor growth. Because overexpression of the trypsin-resistant peptide does not inhibit endogenous c-MYC activity, we conclude that the trypsin-resistant BIN1 peptide contains a

bona fide BIN1 MID domain. This is the first report that provides the structural basis for the cancer suppression mediated by BIN1 in a manner independent of dysregulated c-MYC activity.

Materials and Methods

Cell lines: All cell lines used in this study were purchased from the American Type Culture Collection (ATCC, Manassas, VA) and were maintained in 5% CO_2 at 37°C.

Plasmid DNAs: All spliced isoforms and deletion mutants of human BIN1 cDNAs and the luciferase reporter vectors used in this study have been described previously (Sakamuro *et al.,* 1996; Wechsler-Reya *et al.,* 1997; Elliott *et al.,* 1999; DuHadaway *et al.,* 2001; Kinney *et al.,* 2008; Cassimere *et al.,* 2009; Pyndiah *et al.,* 2011). To express a 6×histidine (His_6)-tagged BIN1 recombinant protein (or His_6-BIN1), the full-length human BIN1 (isoform 8) cDNA was amplified by polymerase chain reaction (PCR) with a set of the following primers: (forward) BIN(Bam) 5′-ATAAGGATCCCGATGGCAGAGATGGGCAGTAAAGGG-3′ and (reverse) 99SH3(Sal) 5′-CAAGTCGACTCATGGGACCCTCTCAGTGAAGTTCTC-3′, under the subsequent reaction conditions: an initial denaturation at 94°C for 1 min; 30 cycles at 94°C for 30 sec, 55°C for 30 sec, and 72°C for 1 min; and a final extension at 72°C for 10 min. The amplified His_6-BIN1 cDNA PCR product was digested with *Bam*HI and *Sal*I and ligated into the pET28c(+) plasmid vector (Novagen, Gibbstown, NJ) to generate the pET28c(+)–His_6-BIN1 plasmid. The nucleotide sequences of the amplified cDNA fragments were verified by DNA sequencing and restriction digestion.

Overexpression of recombinant His_6-BIN1 protein and its purification with column chromatography: The bacterial pellet containing His_6-BIN1 recombinant protein was resuspended in ice-cold buffer A (3 M urea, 1 × phosphate-buffered saline (PBS), pH 8.0), gently lysed by sonication, and centrifuged at 15,000 × g for 45 min at 4°C. The cleared supernatant was loaded onto a 5 ml nickel (Ni) column (GE Healthcare Life Sciences, Pittsburgh, PA), which was pre-equilibrated with buffer A at room temperature (r.t.). After extensive washing with buffer A, the bound fractions were eluted with increasing concentrations of imidazole (80–800 mM) (Sigma-Aldrich, St Louis, MO) in buffer A. The eluted fractions containing His_6-BIN1 proteins with 200 mM imidazole were combined and dialyzed with a 10 kDa dialysis membrane (Pierce, Rockford, IL) into excess buffer A with gently stirring overnight at r.t.

The His_6-BIN1 protein-containing imidazole solution was applied to the Sephacryl S-200 gel filtration chromatography column pre-equilibrated with buffer A at 4°C. Each column fraction was monitored by ultraviolet (UV) absorption at 280 nm and subjected to sodium dodecyl sulfate-polyacrylamide gel electrophoresis (SDS-PAGE) followed by Coomassie Brilliant Blue (CBB R-250) staining. Alternatively, Western analysis with either an anti-His (GE Healthcare Life Sciences) or an anti-BIN1 monoclonal antibody (clone 99D or 2F11) (Santa Cruz Biotechnology, Santa Cruz, CA) was performed.

Limited tryptic digestion: A range-finding experiment was performed to determine the optimum concentration of tosyl phenylalanyl chloromethyl ketone (TPCK)-trypsin (Pierce) for limited protein digestion. After the Sephacryl S-200 gel filtration, His_6-BIN1 protein (approximately 1.0 μg/μl) was mixed with increasing doses of the TPCK-trypsin solution and incubated at r.t. The

concentrations of the TPCK-trypsin we tested were 0, 0.00005, 0.0005, 0.005, 0.05, 0.5, and 5.0 μg/μl. For a time-course experiment, approximately 1/10 (v/v) of the reaction mixture was removed at different time points (0–200 min) and mixed immediately with 1/100 volume of phenyl-methane-sulfonyl-fluoride (PMSF; final concentration 1 mM) to inhibit trypsin. To visualize trypsin-resistant bands after CBB R-250 staining in a protein gel, the concentration of the peptides was increased by vacuum centrifugation.

Edman peptide sequencing: The partially digested His_6-BIN1 peptides were fractionated by 14% SDS-PAGE and blotted onto a PVDF membrane (Millipore, Temecula, CA). The blotted membrane was soaked in deionized water, rinsed in methanol, and stained with 5.0 mg/ml CBB R-250 for 2–4 min in a methanol: glacial acetic acid: distilled water solution (45:10:45 v/v/v). The membrane was rinsed in 50% (v/v) methanol to reduce the background, and subjected to Edman peptide sequencing analysis. The six N-terminal amino acids were determined with the Applied Biosystems Procise 492 Protein Sequencer in the gas-phase mode at the Macromolecular Structure Core Facility, Purdue University, Indiana.

Mass spectrometry: After limited trypsin digestion of a vacuum-concentrated His_6-BIN1 protein, the digested products were fractionated with 14% SDS-PAGE. The peptides in one half of the gel were transferred to a PVDF membrane and stained with CBB R-250. The stained PVDF membrane was placed over the other half of the gel, and the desired peptide band was excised from the acrylamide gel. The gel piece was crushed and washed in distilled water (1 ml) and centrifuged at 15,000 × g for 1 min at r.t. to remove the supernatant. Crushed gel pieces were mixed with 200 μl of formic acid: water: isopropanol (1:3:2 v/v/v) and incubated at r.t. for overnight with gentle

agitation. The sample was centrifuged at 15,000 × g to isolate the supernatant. The total volume was reduced by vacuum centrifugation to approximately 20–30 μl and subjected to mass spectrometric analysis. Mass spectrometric data were obtained with the Voyager Bio-Spectrometry Workstation by Perceptive Biosystems in the Mass Spectrometry Core Facility, Purdue University, Indiana.

***In situ* immunofluorescence analysis**: The primary antibodies were applied to the formaldehyde-fixed cells for 1 h at r.t. After gentle washing with PBS, cells were hybridized with secondary antibodies conjugated with Alexa Fluor 488 (Molecular Probes, Eugene, OR) at r.t. in the dark. The cells were examined with fluorescence microscopy using an Eclipse TE 200 microscope (Nikon, Tokyo, Japan). Hoechst 33342 was used for nuclear counterstaining. The images were recorded with a digital camera (DXM 1200; Nikon) and processed with the imaging software MetaVue (Universal Imaging Co., Downingtown, PA).

Luciferase reporter assay: Luciferase reporter assays were performed as described previously (Kinney *et al.,* 2008; Cassimere *et al.,* 2009). Briefly, 2 μg of luciferase reporter plasmid DNA was transfected into freshly cultured cells in a 6 cm culture dish using FuGENE 6 DNA transfection reagent (Roche Applied Science, Indianapolis, IN), according to the instruction manual. At 48 h after transfection, the luciferase activity was analyzed with a luminometer. To normalize the transfection efficiency, 0.2 μg of pcDNA3–β-galactosidase vector (CMV–β-gal) was cotransfected. Three independent experiments were performed for statistical analysis.

Colony formation suppression assay – Tumor colony formation assays were performed as described previously (Sakamuro *et al.,* 1996; Elliott *et al.,* 1999). Briefly, cells were plated at a density of 1–2 × 10^3 cells/cm^2 in six-well dishes approximately 12–24 h before transfection. Using the FuGENE 6 DNA transfection reagent (Roche Applied Science), 2 μg of the indicated plasmid DNA was transfected, according to the manufacturer's instructions. At 48 h after transfection, the cells were harvested and reseeded into two 6 cm dishes per transfection, followed by selection for 2–3 weeks with 500 μg/ml G418 (Invitrogen, Carlsbad, CA). The G418-resistant colonies were stained and scored with 4% (v/v) Giemsa solution (Invitrogen).

All the cell-based assays described above were repeated independently three times, and the data presented are the means ± standard deviations (SD).

Results

BIN1 splice isoforms suppress tumor colony formation regardless of MBD

We performed *in vitro* colony formation assays. Baker et al (1990) discovered that the wild-type *p53* allele functions as a tumor suppressor in human colorectal carcinoma cells. The *in vitro* colony formation assay has since been considered the most reliable cell-based method to quickly identify a gene that may suppress tumor growth regardless of the mechanism. We first verified that in a dose-dependent manner, ectopically expressed BIN1 suppresses the colony forming activities of a BIN1-deficient breast cancer cell line, MCF7 (Supplementary Fig. S1). Although transient transfection of BIN1 resulted in a robust increase in BIN1 abundance in this

cell line, the stable expression of BIN1 was not detectable in pooled G418-resistant MCF7 colonies, (Supplementary Fig. S2), suggesting that the reduction of G418-resistant colony number after BIN1 transfection is attributable to the cell death activity promoted by BIN1 (Sakamuro *et al.,* 1996; Elliott *et al.,* 1999; DuHadaway *et al.,* 2001). In contrast, it has been suggested that BIN1-associated cell death is silenced in untransformed or nonmalignant cell lines (Sakamuro *et al.,* 1996; Elliott *et al.,* 2000).

There are several spliced isoforms of BIN1, mainly depending on the presence or absence of the peptide sequences encoded by exons 10, 12A, and 13 (Wechsler-Reya *et al.,* 1997; Ge *et al.,* 1999) (Fig. 1A). BIN1 interacts with the c-MYC oncoprotein and inhibits c-MYC–mediated transactivation and transformation via the BIN1 MYC-binding domain (MBD) (Sakamuro *et al.,* 1996; Elliott *et al.,* 1999). Because the MBD region is composed of exons 13 and 14 (Wechsler-Reya *et al.,* 1997), we hypothesized that an exon 13-missing spliced BIN1 isoform, such as BIN1–13 that cannot inhibit c-MYC activity, less efficiently suppresses tumor growth than an exon 13-containing BIN1 that can inhibit c-MYC. Stable transfection of the BIN1 isoforms consistently attenuated colony forming activities of MCF7 cells, regardless of the presence or absence of exons 10, 12A, and/or 13 (Figs. 1B & C). Essentially the same result was obtained with some other BIN1-sensitive cancer cell lines, such as LNCaP prostate cancer line (Supplementary Fig. S3). As predicted, none of the spliced BIN1 isoforms displayed growth inhibition in the human untransformed breast epithelial cell line, MCF10A (Figs. 1B & C). We concluded that BIN1 functions as a cancer suppressor through the region that commonly exists in all spliced isoforms of BIN1 (Fig. 1A, *underlined*).

Elliott *et al.,* (1999) showed that the deletion of the C-terminal half of the BIN1 BAR region (designated BAR-C), but neither the deletion of MBD nor SH3, compromises BIN1-mediated cancer suppression, suggesting that the BAR-C region might contain a BIN1 effector domain. Our colony-formation assays also demonstrated that the BIN1 BAR-N region is as important as the BAR-C region (Supplementary Fig. S4). These independent studies consistently show that the BIN1 BAR region is essential for BIN1-mediated cancer suppression. However, because the separation of the BAR-N and BAR-C regions is artificial, and is not based on structural evidence, deletion of either the BAR-N or BAR-C region might disrupt the proper folding of the entire BIN1 protein, thereby masking or embedding the *bona fide* effector domain of BIN1. Furthermore, an artificial deletion could reduce the stability of the protein. Consistent with this possibility, the amount of ectopically expressed BAR-C-deleted BIN1 protein (BIN1ΔBAR-C) was greatly reduced *in vivo*, but was not affected *in vitro* (Supplementary Fig. S5). Therefore, the loss of BIN1-mediated tumor suppression caused by an artificial BAR deletion might be simply attributable to a reduction in BIN1 abundance *in vivo*. To identify the naturally folded effector domain of BIN1, we undertook limited proteolytic digestion of the recombinant full-length BIN1 protein.

BIN1 contains a peptide sequence that is resistant to limited trypsin digestion

Stably folded domain structures are expected to be more resistant to limited protease digestion than unfolded flexible linker regions (Fontana *et al.,* 1997). Therefore, if a region of a protein of interest is resistant to limited proteolysis, the region might contain a naturally folded domain structure. We purified the human recombinant full-length BIN1 protein as the substrate for

limited proteolytic digestion. The N-terminal 6×histidine (His_6)-tagged BIN1 (isoform 8) protein (His_6-BIN1) was overexpressed in *Escherichia coli* BL21 (DE3) (Fig. 2A, *lane 1*). Lower molecular weight proteins (28-50 kDa) were copurified with high levels of full-length His_6-BIN1 (70 kDa band) by nickel (Ni)-affinity column chromatography (Fig. 2A, *lane 2*). These copurified short peptides might represent histidine-rich bacterial proteins or C-terminal truncated forms of His_6-BIN1 and were removed with a Sephacryl S-200 gel filtration column (Fig. 2A, *lane 3*). The protein concentration in each eluted fraction was monitored during gel filtration by ultraviolet (UV) absorption at 280 nm. The presence and purity of the full-length His_6-BIN1 protein in each eluted fraction were verified by a protein gel stained with Coomassie Brilliant Blue (CBB). The full-length His_6-BIN1 fractions from tube #25 to #27 were combined as a substrate for limited tryptic digestion (Supplementary Fig. 6). The presence of His_6-BIN1 protein (~70 kDa) was also verified by Western analysis with an anti-His or an anti-BIN1 (clone 99D) antibody (data not shown). The final yield of His_6-BIN1 was approximately 7% (w/w).

For the limited proteolysis of purified His_6-BIN1, we used tosyl phenylalanyl chloromethyl ketone (TPCK)-treated trypsin, which deactivates residual chymotrypsin activity and cleaves on the carbonyl side of lysine and arginine residues unless they are immediately followed by proline. There are 42 lysine and 17 arginine residues amongst the 454 amino acids of BIN1 (isoform 8), none of which are followed by proline (Sakamuro *et al.,* 1996). To determine the optimal concentration of TPCK-trypsin for limited proteolysis, serially diluted protease solutions were mixed with a constant amount of His_6-BIN1 protein (20 μg) and incubated at room temperature (r.t.) for 10 min. Partial digestion of His_6-BIN1 protein should occur under an optimal proteolytic

condition, leaving some full-length His_6-BIN1 protein intact. Accordingly, a concentration of 0.005 μg/μL TPCK-trypsin was determined to be optimal (Fig. 2B).

We next performed time-course experiments of trypsin digestion and determined the experimental condition at which partial cleavage of His_6-BIN1 protein by trypsin occurred. In the optimized condition, partially digested His_6-BIN1 bands should remain resistant at least for a while. As shown in Fig. 2C, a peptide band (~15 kDa) initially appeared after 20 min incubation and it was not fully digested after 100 min. The intensity of the 15-kDa peptide band gradually increased during 50 min of tryptic digestion, and then decreased to 100 min. The accumulation of the 15-kDa peptide during incubation with 0.005 μg/μL TPCK-trypsin for up to 50 min suggests that this peptide fragment is somewhat resistant to limited trypsin digestion. Therefore, we assumed that the ~15 kDa BIN1 peptide fragment retains a folded structure by which the peptide could be protected from limited tryptic digestion.

The 15-kDa BIN1 peptide encompasses part of the BAR-C region

To determine the N-terminal boundary of the 15-kDa tryptic BIN1 peptide, partially digested His_6-BIN1 protein by TPCK-trypsin was subjected to sodium dodecyl sulfate polyacrylamide gel electrophoresis (SDS-PAGE) and the tryptic peptides on a protein gel were electronically transferred to a polyvinylidene difluoride (PVDF) membrane. A broad protein band at approximately 15 kDa was excised from the membrane and was subjected to Edman peptide sequencing (Supplementary Fig. S7). Three independent trials for Edman degradation consistently revealed a six-amino acid sequence, lysine-leucine-valine-aspartic acid-tyrosine-aspartic acid

(KLVDYD), which corresponded to residues 146–151 of BIN1 (isoform 8). Interestingly, essentially the same sequence, ^{146}KLVDY^{150}, was previously identified empirically when a minimal region of the BAR-C region that is essential for BIN1-mediated tumor suppression was determined (Elliott *et al.,* 1999; DuHadaway *et al.,* 2001). The coincidence of the amino acid sequences in these two separate experiments suggests that the ^{146}KLVDY^{150} sequence is critical for sustaining the proper structure and function of BIN1. We concluded that lysine^{146} can be the N-terminal residue of the 15-kDa BIN1 tryptic peptide.

We next determined the C-terminal end of the 15-kDa peptide. To do this, we analyzed the exact mass of the tryptic peptide. The broad 15-kDa band was extracted from a protein gel and was subjected to mass spectrometric analysis. The shapes of mass peaks were broad probably because of micro heterogeneity of the tryptic peptides, and there were one major peak, which was identified with a mass of 13,559.8 (*peak 1*), together with two minor peaks with masses of 10,996.0 (*peak 2*) and 9270.6 (*peak 3*) (Supplementary Fig. S8). We focused on the analysis of *peak 1*, because this was both the major peak and the peak of greatest molecular size. Given that the 15-kDa BIN1 peptide commences from lysine^{146} (see above), the most likely C-terminal boundary of the peptide, which is consistent with the theoretical mass values of *peak 1*, is arginine^{263} (Fig. 3A, *asterisk*). However, arginine^{263} exists in the middle of unique region-3 (U3) (Fig. 3A, *underlined*), which is tightly associated with BIN1-mediated cellular differentiation and growth arrest (Wechsler-Reya *et al.,* 1998). Because the U3 region contains multiple lysine and arginine residues (Fig. 3A, *underlined*), we wondered whether the U3 region might be easily digested with limited amounts of trypsin, even though the U3 region likely composes part of a folded domain structure. For that reason, we propose lysine^{268}, which is the most C-terminal potentially trypsin-sensitive site in the

U3 region, as the C-terminal residue of the 15-kDa peptide. Collectively, we concluded that the 15-kDa BIN1 peptide encompasses the region between lysine^{146} and lysine^{268}.

The 15-kDa BIN1 peptide contains a unique coiled-coil structure

This region partially includes the BAR-C region, a putative tumor-suppressive domain of BIN1 (Elliott *et al.,* 1999, 2000), and is completely separate from MBD (Sakamuro *et al.,* 1996). To gain further insights into the structure of the 15-kDa peptide, we used several computer server programs that predict the secondary and tertiary structure. First, computational analysis with the PSIPRED program (McGuffin *et al.,* 2000) revealed that lysine^{146} (Fig. 3A, *sharp symbol*) is located in the middle of an α-helix (Fig. 3A, *rectangle*). The COILS server (Lupas *et al.,* 1991) predicted that highly coiled-coil regions are present within the tryptic 15-kDa peptide (Fig. 3B). The Paircoil2 server (McDonnell *et al.,* 2006) provided consistent results with the COILS server, predicting essentially the same coiled-coil structure for the 15-kDa fragment (D.K. and D.S., unpublished observation). In addition to α-helices and β-strands, several turns were also expected by a series of prediction servers that use neural networks (Kaur and Raghava, 2003a, 2003b). Together, the computer-based predictions of the secondary structure suggest that coiled-coil structural motifs are most likely located within the 15-kDa peptide fragment of BIN1 (Fig. 3B).

The crystal structure of part of the human BIN1 BAR region has been determined (Casal *et al.,* 2006). Because the 15-kDa peptide encodes part of the BAR-C region, we mapped the 15-kDa peptide sequence onto the three-dimensional (3-D) X-ray structure of the BIN1 BAR fragment (PDB accession number 2FIC). To do this, we used the Cn3D 4.1 program (Hogue, 1997).

Interestingly, the N-terminal sequence of the 15-kDa peptide, ^{146}KLVDY^{150}, lied on the boundary between the double- and triple-coiled-coil domains of the BIN1 BAR region (Fig. 3C, *turquoise*), indicating again that the KLVDY sequence may play a critical role in sustaining the structure and function of BIN1. Furthermore, LOMETS (Local Meta-Threading-Server) program, which predicts the 3-D structure of a protein (Wu and Zhang, 2007), verified that highly coiled-coil motifs of BIN1 exist within the 15-kDa peptide-coding region (Fig. 3D). We concluded that the 15-kDa peptide contains a unique coiled-coil structure by which the 15-kDa region might be protected from limited tryptic digestion.

The 15-kDa BIN1 peptide attenuates tumor growth in a manner independent of c-MYC

To establish the biological effect of the 15-kDa BIN1 peptide on cultured cancer cells, the expression vector that encodes a hemagglutinin (HA)-tagged tryptic 15-kDa peptide (designated HA-Trp) was transfected into two BIN1-sensitive human cancer cell lines, MCF7 and LNCaP. The heterologously expressed HA-Trp peptide inhibited tumor colony formation as efficiently as the full-length BIN1 protein (Fig. 4A), suggesting that the 15-kDa peptide is sufficient to attenuate tumor growth. Although transiently expressed HA-Trp was detectable in tumor cells, we were not able to obtain stably-transfected tumor cells that constitutively express the HA-Trp peptide (E.L.K., S. T. and D.S., unpublished observation). This observation further supports the potential growth-suppressive properties of this peptide. To determine whether the HA-Trp-mediated growth-suppression is independent of c-MYC activity, the HA-Trp-expression vector was cotransfected with the E-box MYC-binding Sequence (EMS)-luciferase reporter. The EMS-Luc can be specifically activated by endogenous and exogenous c-MYC (Kinney *et al.,* 2008). As positive and

negative controls for the c-MYC inhibition, the full-length BIN1 and HA-tagged BIN1ΔMBD expression vectors were cotransfected, respectively. BIN1 inhibited endogenous c-MYC-mediated EMS-Luc activity, whereas either HA-BIN1ΔMBD or HA-Trp peptide did not (Fig. 4B). Interestingly, similar to the HA-BIN1ΔMBD polypeptide (Pyndiah *et al.,* 2011), the HA-Trp peptide was present largely in the cytoplasm. In contrast, transfected BIN1 was detected exclusively in the nucleus in two BIN1-deficient cell lines, MCF7 and DU145. Hoechst staining and endogenous PARP1 proteins were used as the positive controls for the nuclear localization (Pyndiah *et al.,* 2011) (Fig. 4C). Our results suggest that the trypsin-resistant 15-kDa peptide encodes a MYC-independent *bona-fide* effector domain (MID), through which BIN1 acts as a c-MYC-independent tumor suppressor.

Discussion

Structure–function studies of artificial deletion mutants of the BIN1 tumor suppressor demonstrated that the N-terminal BAR region, a domain that allows the binding or twisting of the BIN1 protein (Habermann, 2004), contains the tumor-suppressive effector function (Elliott *et al.,* 1999, 2000). However, precisely which domain of the BAR region is sufficient for BIN1-mediated cancer suppression remained unclear. Although artificial deletion mutants are widely used for functional cell-based studies, the structural integrity for a deleted peptide fragment *per se* and the functional activities of the remaining polypeptide require careful validation. In this respect, limited proteolysis is a reasonable method with which to search for an undefined domain structure in functionally important, but structurally ambiguous proteins.

In this study, we undertook limited tryptic digestion of the human full-length BIN1 protein, and the structure and function of the trypsin-resistant BIN1 peptide were analyzed with Edman sequencing, mass spectrometry, computational structural prediction, and cell-based assays. We identified a coiled-coil BIN1 BAR region as a novel BIN1 MYC-independent effector domain (MID) for cancer suppression. Because the BIN1 MID-containing region, which includes part of the BAR-C region, was not subject to alternative splicing (Fig. 1A, *underlined*), we propose that the BIN1 MID region may be responsible, at least in part, for the tumor-suppressor activity of the spliced isoforms of BIN1 protein, which are ubiquitously expressed. Our finding also revealed the growth-inhibitory property of the BIN1 MID peptide itself, regardless of any dysregulated c-MYC activity. This finding is potentially significant because it suggests that the MID region contains a *bona fide* BIN1 effector domain for cancer suppression. Given that the overexpression or deregulated expression of c-MYC is among the hallmarks of human malignancies (Meyer & Penn, 2008), the BIN1 MID peptide may have utility as a novel intervention for the treatment of human cancers that overexpress c-MYC.

The ectopically expressed BIN1ΔMBD polypeptide existed stably in the cytoplasm and acted as a tumor suppressor without inhibiting c-MYC-mediated oncogenic transactivation (Sakamuro *et al.*, 1996; Elliott *et al.,* 1999; Pyndiah *et al.,* 2011). Similarly, the heterologously expressed BIN1 MID peptide fragment was predominantly detected in the cytoplasm and was sufficient to inhibit tumor cell proliferation without attenuating c-MYC activity (Fig. 4). This coincidence may be explained by the fact that the BIN1ΔMBD polypeptide contains an intact MID sequence. Furthermore, some spliced BIN1 isoforms, which exist mainly in the cytoplasm, contain

the MID peptide and act as growth suppressors. For example, a spliced BIN1 isoform that is associated with the differentiation of the skeletal muscle exists in the cytoplasm and is essential for the growth arrest of differentiated skeletal muscle cells, in which endogenous c-MYC is undetectable (Wechsler-Reya *et al.,* 1998). These results suggest that if the MID-containing BIN1 polypeptide functions in the cytoplasm, it must have an activity that does not directly involve the inhibition of c-MYC, which occurs in the nucleus. In contrast, a number of BIN1 isoforms are normally present in the nucleus and act as cancer suppressors, regardless of deregulated c-MYC activity (Sakamuro et al. 1996; Wechsler-Reya et al. 1997), suggesting that the BIN1 MID region may also interact with a non-MYC effector protein in the nucleus.

The most fascinating feature of the BIN1-mediated cellular function is its antiproliferative property, which is only observed in tumor cells, and not in untransformed cells (Fig. 1C). This is particularly intriguing because it suggests the possible development of a cancer-selective therapeutic intervention involving BIN1, with little or no adverse effects on the normal peripheral tissues. Although it is unclear how BIN1 selectively exerts its antiproliferative function on tumor cells, the interaction between the BIN1 MID region and its effector protein in the nucleus or cytoplasm may only occur in tumor cells. Alternatively, the BIN1 MID region may be masked or occupied by a silencer protein in untransformed cells. In either model, it will be interesting in future studies to identify MID-interacting cytoplasmic and nuclear proteins that may act as critical BIN1 effector (or silencer) proteins in cancer suppression.

Acknowledgments

We thank Melissa D. Zolodz for technical assistance with mass spectrometry. This work was supported by the Wendy Will Case Cancer Fund, the Louisiana Cancer Research Consortium Funds, the DOD Prostate Cancer Research Award (DAMD 17-02-10131), and the Susan G. Komen Breast Cancer Foundation (to D.S.), and partly by the National Center for Research Resources (P20RR021970). D.K. was the recipient of the NIH R01GM075004, the NSF DMS0604776, DMS0800568, EF0850009, and IIS0915801; G.L.L, a Kienly Teaching Assistant Award; N.E.D., a Coca-Cola Fellowship; and E.K.C., a Bowen Fellowship, a Purdue Research Foundation Predoctoral Fellowship, and an NIH-sponsored Predoctoral Fellowship (1F31CA110205-01).

References

Baker SJ, Markowitz S, Fearon ER, Willson JK & Vogelstein B (1990) Suppression of human colorectal carcinoma cell growth by wild-type p53. *Science* **249** (4971), 912-915.

Brzovic PS, Meza J, King MC & Klevit RE (1998) The cancer-predisposing mutation C61G disrupts homodimer formation in the NH_2-terminal BRCA1 RING finger domain. *J Biol Chem* **273** (14), 7795-7799.

Casal E, Federici L, Zhang W, Fernandez-Recio J, Priego EM, Miguel RN, DuHadaway JB, Prendergast GC, Luisi BF & Laue ED (2006) The crystal structure of the BAR domain from human BIN1/amphiphysin II and its implications for molecular recognition. *Biochemistry* **45** (43), 12917-12928.

Cassimere EK, Pyndiah S & Sakamuro D (2009) The C-MYC-interacting proapoptotic tumor suppressor BIN1 is a transcriptional target for E2F1 in response to DNA damage. *Cell Death & Diff* **16** (12), 1641-1653.

DuHadaway JB, Sakamuro D, Ewert DL & Prendergast GC (2001) BIN1 mediates apoptosis by C-MYC in transformed primary cells. *Cancer Res* **61** (7), 3151-3156.

Elliott K, Sakamuro D, Basu A, Du W, Wunner W, Staller P, Gaubatz S, Zhang H, Prochownik E, Eilers M & Prendergast GC (1999) BIN1 functionally interacts with c-MYC and inhibits cell proliferation via multiple mechanisms. *Oncogene* **18** (24), 3564-3573.

Elliott K, Ge K, Du W, & Prendergast GC (2000). The c-Myc-interacting adaptor protein Bin1 activates a caspase-independent cell death program. *Oncogene* **19** (41), 4669-4684.

Fontana A, Zambonin M, De Filippis V, Bosco M & Polverino de Laureto P (1995) Limited proteolysis of cytochrome c in trifluoroethanol. *FEBS Lett* **362** (3), 266-270.

Fontana A, Polverino de Laureto P, De Filippis V, Scaramella E & Zambonin M (1997) Probing the partly folded states of proteins by limited proteolysis. *Fold Des* **2** (2), R17-R26.

Ge K, DuHadaway J, Du W, Herlyn M, Rodeck U & Prendergast GC (1999) Mechanism for elimination of a tumor suppressor: aberrant splicing of a brain-specific exon causes loss of function of BIN1 in melanoma. *Proc Natl Acad Sci USA* **96** (17), 9689-9694.

Ge K, Minhas F, DuHadaway J, Mao NC, Wilson D, Buccafusca R, Sakamuro D, Nelson P, Malkowicz SB, Tomaszewski J & Prendergast GC (2000) Loss of heterozygosity and tumor suppressor activity of Bin1 in prostate carcinoma. *Int J Cancer* **86**, 155-161.

Habermann B (2004) The BAR-domain family of proteins: a case of bending and binding? *EMBO Rep* **5** (3), 250-255.

Hogue CW (1997) Cn3D: a new generation of three-dimensional molecular structure viewer. *Trends Biochem Sci* **22** (8), 314-316.

Kamath N, Karwowska-Desaulniers P, Pflum MK. (2006) Limited proteolysis of human histone deacetylase 1. *BMC Biochem* **7**, 22.

Kameshita I, Matsuda M, Nishikimi M, Ushiro H & Shizuta Y (1986) Reconstitution and poly(ADP-ribosyl)ation of proteolytically fragmented poly(ADP-ribose) synthetase. *J Biol Chem* **261** (8), 3863-3868.

Kaur H & Raghava GP (2003a) Prediction of beta-turns in proteins from multiple alignment using neural network. *Protein Sci* **12** (3), 627-634.

Kaur H & Raghava GP (2003b) A neural-network based method for prediction of gamma-turns in proteins from multiple sequence alignment. *Protein Sci* **12** (5), 923-929.

Kinney EL, Tanida S, Rodrigue AA, Johnson JK, Tompkins VS & Sakamuro D (2008) Adenovirus E1A oncoprotein liberates C-MYC activity to promote cell proliferation through abating BIN1 expression via an Rb/E2F1-dependent mechanism. *J Cell Physiol* **216** (3), 621-631.

Lupas A, Van Dyke M & Stock J (1991) Predicting Coiled Coils from Protein Sequences. *Science* **252** (5010), 1162-1164.

McDonnell AV, Jiang T, Keating AE & Berger B (2006) Paircoil2: Improved prediction of coiled coils from sequence. *Bioinformatics* **22** (3), 356–358.

McGuffin LJ, Bryson K & Jones DT (2000) The PSIPRED protein structure prediction server. *Bioinformatics* **16** (4)**,** 404-405.

Meyer N & Penn LZ (2008) Reflecting on 25 years with C-MYC. *Nat Rev Cancer* **8** (12), 976-999.

Pineda-Lucena A, Ho CS, Mao DY, Sheng Y, Laister RC, Muhandiram R, Lu Y, Seet BT, Katz S, Szyperski T, Penn LZ & Arrowsmith CH (2005) A structure-based model of the C-MYC/BIN1 protein interaction shows alternative splicing of BIN1 and C-MYC phosphorylation are key binding determinants. *J Mol Biol* **351** (1), 182-194.

Prendergast GC, Muller AJ, Ramalingam A & Chang MY (2009) BAR the door: cancer suppression by amphiphysin-like genes. *Biochim Biophys Acta* **1795** (1), 25-36.

Pyndiah S, Tanida S, Ahmed KM, Cassimere EK, Choe C & Sakamuro D (2011) c-MYC suppresses BIN1 to release poly(ADP-ribose) polymerase 1: a mechanism by which cancer cells acquire cisplatin resistance. *Sci Signal* **4**, ra19.

Sakamuro D, Elliott KJ, Wechsler-Reya R & Prendergast GC (1996) BIN1 is a novel C-MYC-interacting protein with features of a tumour suppressor. *Nat Genet* **14** (1), 69-77.

Sakamuro D & Prendergast GC (1999) New C-MYC-interacting proteins: a second C-MYC network emerges. *Oncogene* **18** (19), 2942-2954.

Wechsler-Reya R, Sakamuro D, Zhang J, DuHadaway J & Prendergast GC (1997) Structural analysis of the human BIN1 gene. Evidence for tissue-specific transcriptional regulation and alternate RNA splicing. *J Biol Chem* **272** (50), 31453-31458.

Wechsler-Reya R, Elliott KJ & Prendergast GC (1998) A role for the putative tumor suppressor BIN1 in muscle cell differentiation. *Mol Cell Biol* **18** (1), 566-575.

Wu S & Zhang Y (2007) LOMETS: A local meta-threading-server for protein structure prediction. *Nucl Acids Res* **35** (10), 3375-3382.

Figure Legends

Figure 1 **Effects of BIN1 spliced isoforms on the colony forming activities of MCF7 and MCF10A cell lines. (A)** Alternatively spliced isoforms of BIN1. The BIN1 protein is encoded by 16 exons. The BAR region is encoded by exons 1–8, U1 is encoded by exon 9, U3 is encoded by exon 10, U2 is encoded by exon 11, MBD is encoded by exons 13–14, and the SH3 domain is encoded by exons 15–16. Exon 12A has been detected in brain-specific transcripts (Wechsler-Reya *et al.,* 1997) and metastatic melanoma cells (Ge at al. 1999). Horizontal bars indicate the common regions among the spliced isoforms. **(B)** Morphologies of MCF7 breast cancer and MCF10A untransformed breast epithelial cell lines after the formation of G418-resistant colonies. Growing MCF7 cells and MCF10A cells were stably transfected with the G418-resistant gene-expression vectors that encode indicated cDNAs of the human BIN1 splice isoforms, selected for 14 days and 21 days in G418 (500 μg/ml and 600 μg/ml)-containing growth medium, respectively, and stained with 4% (v/v) Giemsa (Invitrogen). **(C)** Giemsa-stained colonies of indicated cell lines were scored. The numbers of colonies transfected with the empty control vector were used as the positive control. The bars represent the means of three independent experiments ± SD.

Figure 2 **Optimization of limited tryptic digestion of the human recombinant BIN1 protein, His_6-BIN1. (A)** A 30 μl aliquot of each fraction was subjected to 10% SDS-PAGE and stained with CBB R-250. The arrow indicates His_6-BIN1 (~70 kDa). i) *Escherichia coli* lysates containing approximately 70 μg of crude protein; ii) post-Ni column fraction, containing approximately 15 μg of protein; and iii) post-Sephacryl S-200 gel filtration fraction, containing approximately 5 μg of protein. **(B)** Range-finding experiments for tryptic digestion of His_6-BIN1

protein confirmed that 0.005 μg/μl (*asterisk*) was the optimal concentration of TPCK-trypsin for limited trypsinization of His_6-BIN1 protein. **(C)** Time-course experiments for the tryptic digestion (0.005 μg/μl) of His_6-BIN1 protein. The arrow and arrowhead indicate His_6-BIN1 (approx. 70 kDa) and a BIN1 small peptide resistant to trypsin (approximately 15 kDa), respectively. Each aliquot was subjected to 14% SDS-PAGE and CBB staining. The procedures to purify the 15-kDa band were repeated at least three times to confirm the chromatographic reproducibility.

Figure 3 **Identification and characterization of a BIN1 15-kDa peptide registrant to limited trypsin digestion. (A)** Secondary structure prediction of BIN1. The PSIPRED program was used for the secondary structure prediction (McGuffin *et al.,* 2000). The predicted helices and β-strands are presented as rectangles and ellipses, respectively. The region encoding the 15-kDa peptide is highlighted in red. The region indicated by arrows (E_{42}–L_{239}) corresponds to part of the human BIN1 BAR fragment, the three-dimensional structure of which is available *online* under the Protein Data Bank (PDB) accession number 2FIC (Casal *et al.,* 2006). $Leucine_{55}$ (L_{55}), highlighted in a dark green circle, is a microsatellite mutation detected in a set of prostate cancer tissues (Ge *et al.,* 2000). The KLVDY sequence necessary for BIN1-mediated anti-transforming activity is underlined in turquoise (DuHadaway *et al.,* 2001). The region encoding U3 (or exon 10) is underlined in black. $Arginine_{263}$ (*asterisk*) is the calculated C-terminal residue of the BRT fragment. **(B)** Prediction of the coiled-coil region in BIN1. The COILS server (Lupas *et al.,* 1991) was used to predict the coiled-coil regions. The x-axis depicts the amino acid positions in the human BIN1 (isoform 8) protein and the y-axis shows the possibility of coiled-coil regions. The color denotes the window size used in the search. Three BIN1 polypeptides, the 15-kDa peptide (*yellow*), the BIN1 BAR (2FIC) fragment (Casal *et al.,* 2006), and full-length BIN1 (isoform 8;

454 amino acids) (Sakamuro *et al.,* 1996) were aligned. The KLVDY sequence is highlighted in *turquoise*. **(C)** The three-dimensional structure of the 15-kDa peptide (*yellow*) was modeled based on the structure of the human BIN1 BAR fragment (PDB accession number 2FIC), starting from E_{42} through to L_{239} (Casal *et al.,* 2006). The KLVDY sequence, which is the N-terminus of the 15-kDa peptide fragment, is highlighted in *turquoise*. Double and triple coiled-coil domains are indicated with vertical bars, and loops with horizontal bars. The L_{55} residue in dark green corresponds to the location of a satellite mutation found in a set of patients with prostate cancer, as described previously (Ge *et al.,* 2000). Residues D_{93}, T_{162}, and L_{239} are expected to exist in the hinge regions. **(D)** LOMETS (Local Meta-Threading-Server) program (Wu and Zhang, 2007) was used to predict the 3-D structure of the full-length BIN1 protein (*left*) and the 15-kDa peptide (*right*).

Figure 4 **The 15-kDa peptide encodes the BIN1 MYC-independent effector domain (MID) for cancer suppression**. **(A)** Colony formation suppression assays. LNCaP and MCF cancer cell lines were transfected with CMV-BIN1 (2.0 μg) or CMV-HA-Trp (2.0 μg). At 24 h after transfection, the cells were trypsinized and reseeded at a low density in standard growth medium containing G418 at 500 μg/ml. G418-resistant colonies of each cell line were stained and scored after two weeks of drug selection. The data presented are the percentages of colonies formed in the presence of G418 compared to the empty vectors. The bars represent the means of three experiments ± SD. **(B)** The EMS-Luc vector is a c-MYC-responsive reporter construct that contains four tandem repeats of the E-box sequence (*small open dotes*) followed by the SV40 minimal promoter (*top*). EMS–Luc (1.0 μg) reporter vector was cotransfected with 1.0 μg of pLPC empty vector, pLPC-BIN1, pLPC-BIN1ΔMBD, or pLPC-HA-Trp in proliferating LNCaP cells.

The cells were harvested 48 h after transfection for the luciferase assays (*bottom*). Three independent transfections were performed for statistical analysis. **(C)** *In situ* immunofluorescence microscopy verified the cytoplasmic localization of transfected HA-BIN1ΔMBD and HA-Trp polypeptides and the nuclear localization of transfected BIN1 and endogenous PARP1 proteins in two BIN1-deficient cancer cell lines, MCF7 and DU145.

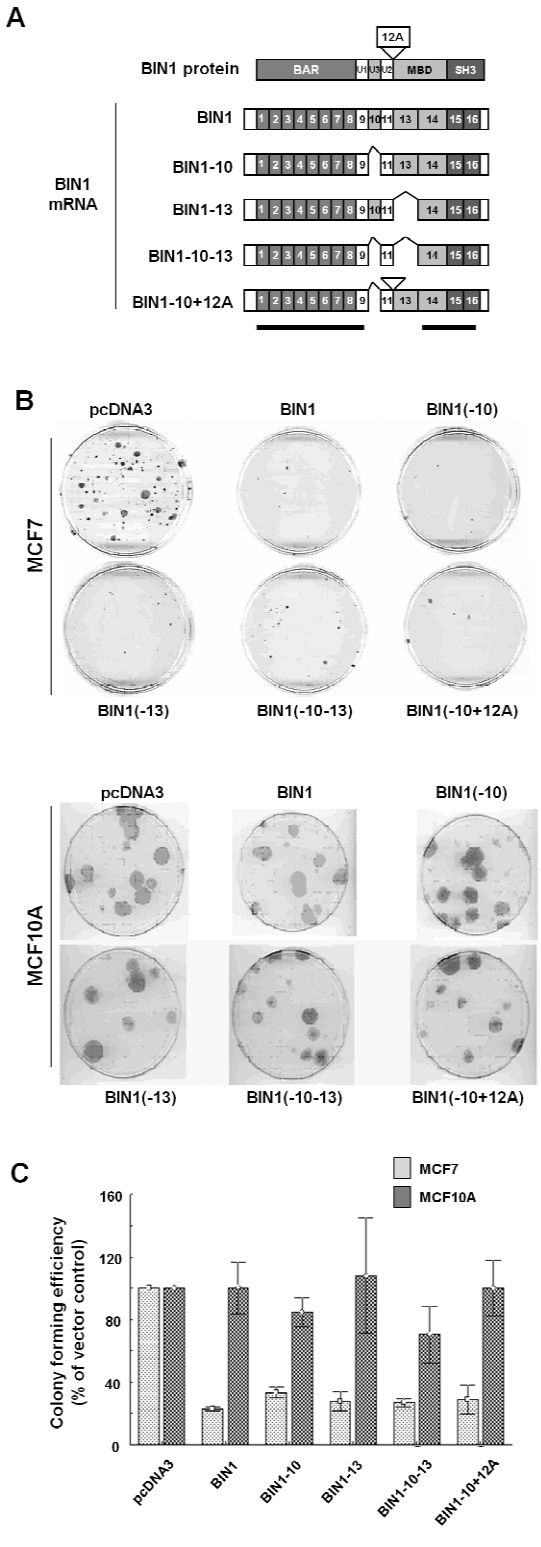

Figure 1

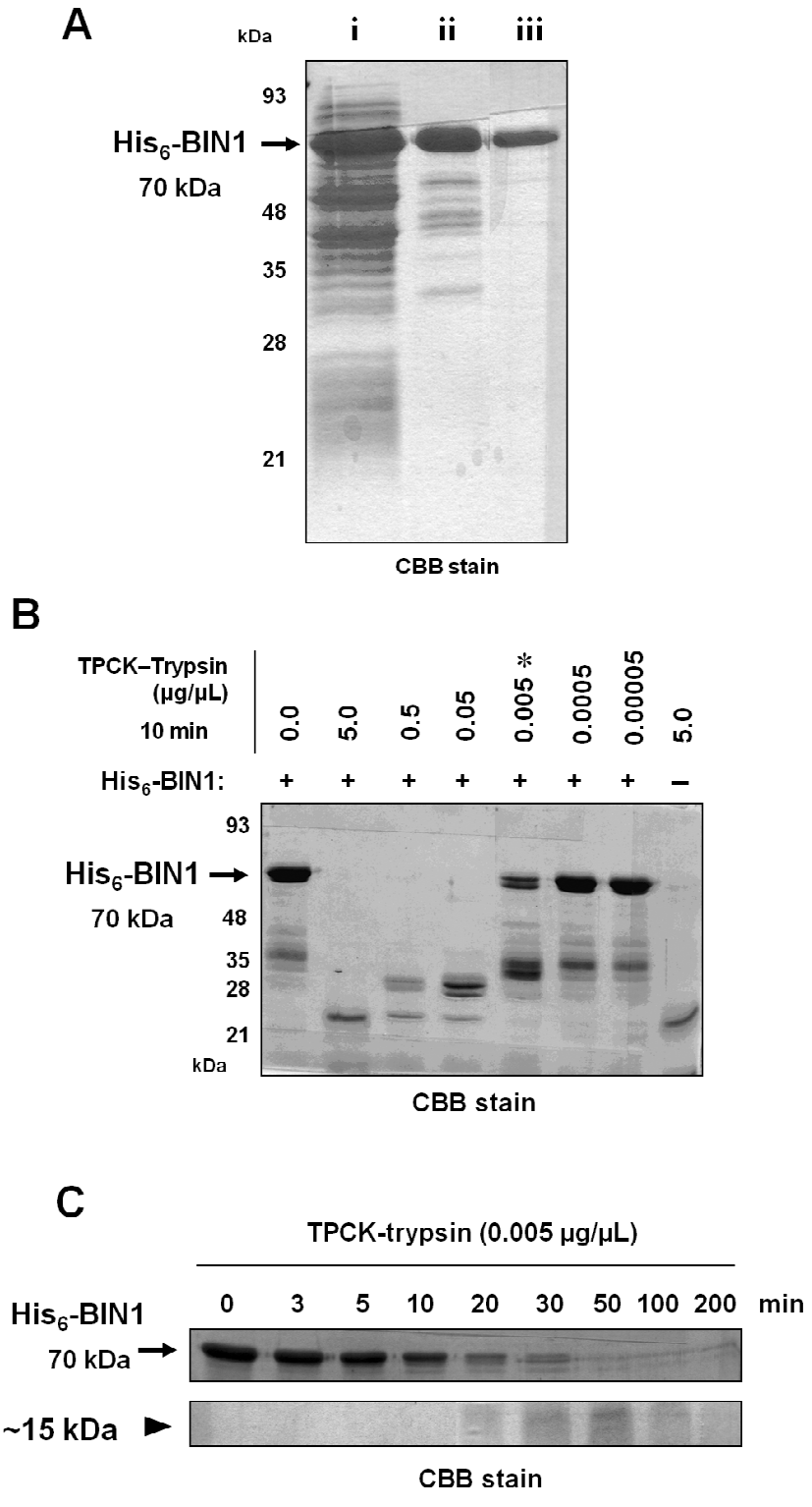

Figure 2

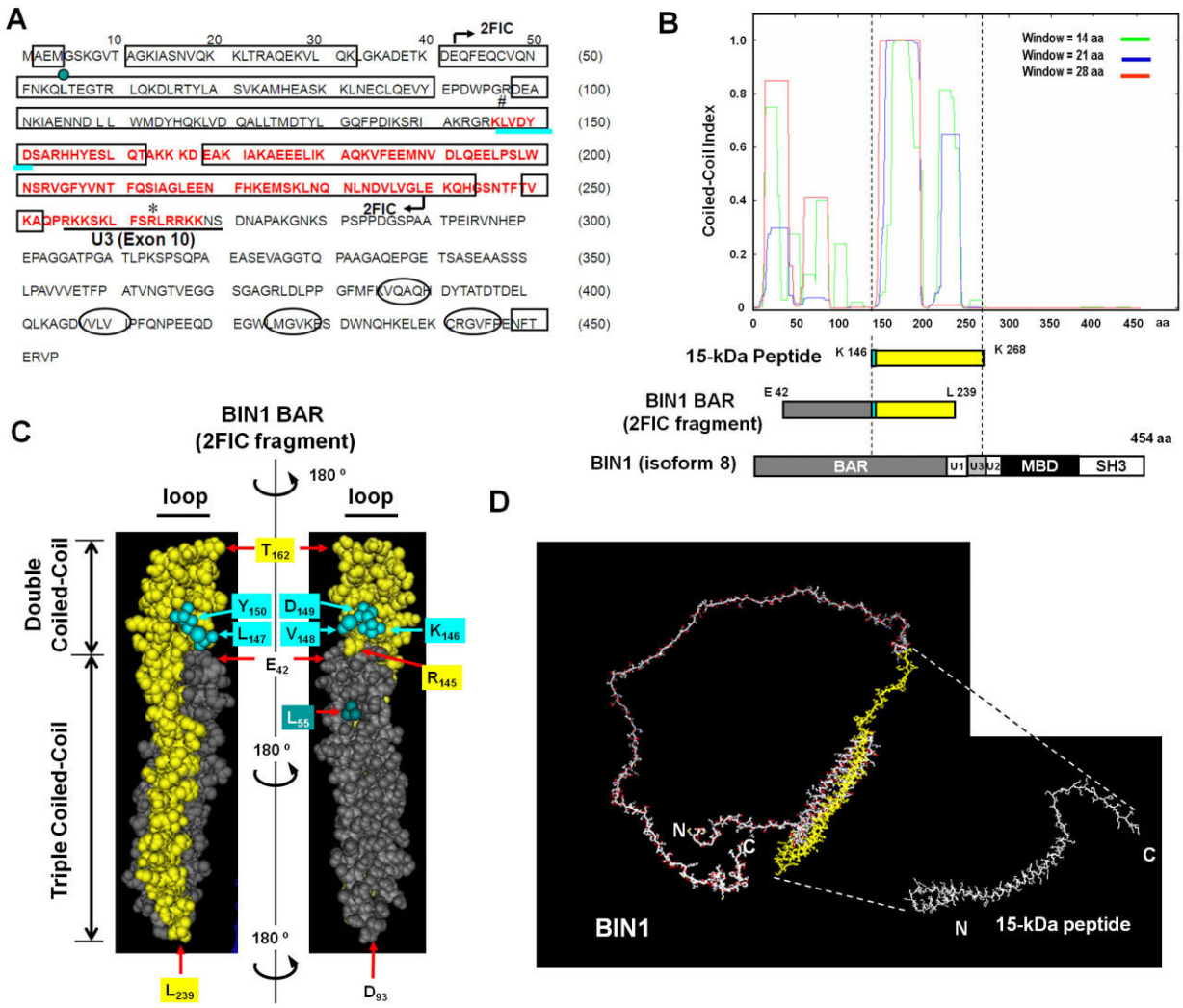

Figure 3

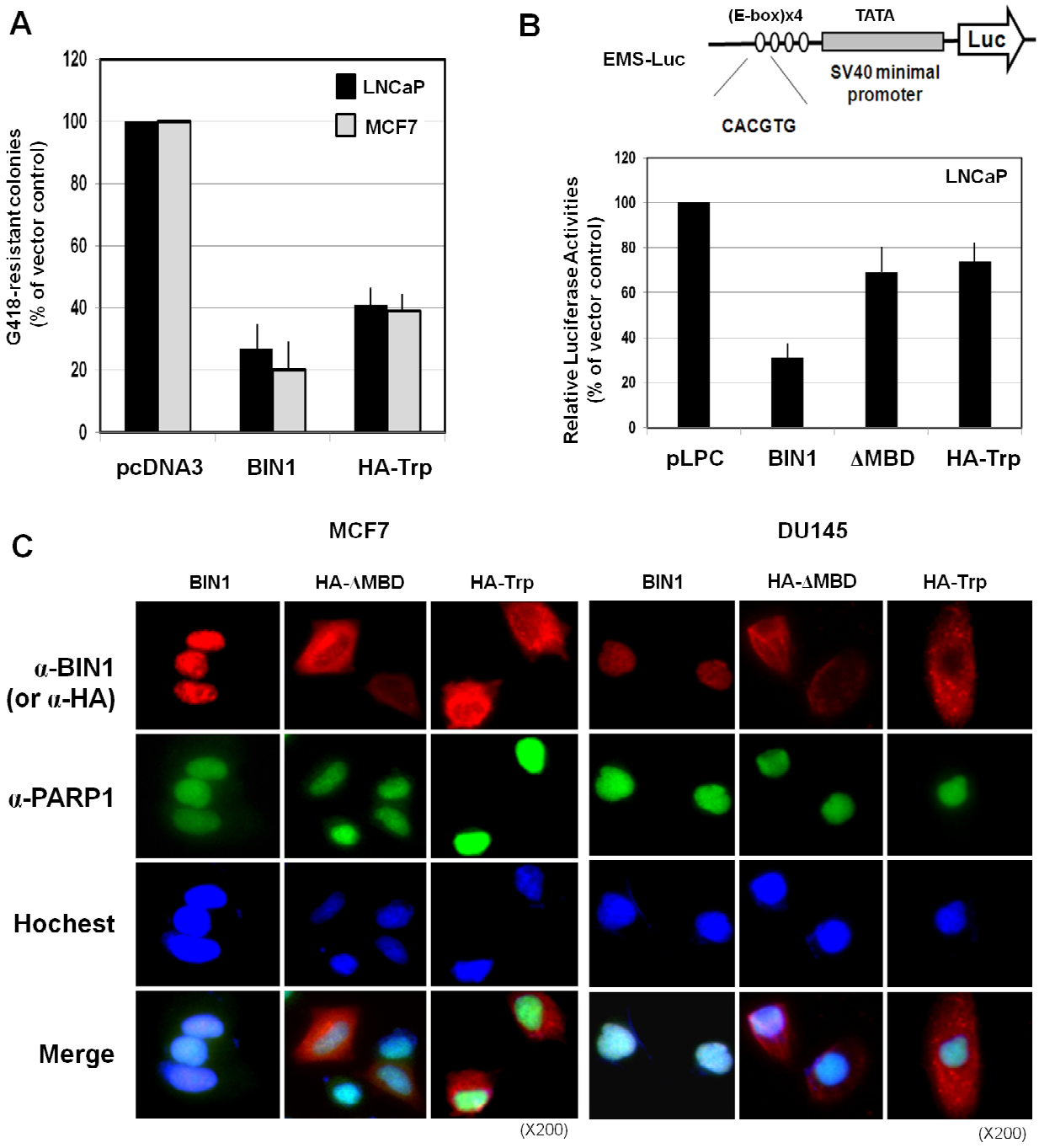

Figure 4